Broadband Characterization of Antennas

Zbyněk RAIDA, Petr ŠMÍD, Jaroslav LÁČÍK, Zbyněk LUKEŠ, Milan MOTL

Dept. of Radio Engineering
Brno University of Technology
Purkyňova 118, CZ-61200 Brno
CZECH REPUBLIC

Abstract: In this paper, we search for a suitable way of characterizing antennas in a wide band of frequencies. First, a canonical antenna is characterized by conventional parameters in frequency domain (directivity pattern, gain, input impedance) on each separate harmonics, and their mean-value counterparts are formulated and discussed. Second, the analysis is performed in the time domain, and following the frequency domain characterization, time-domain parameters are formulated. The correspondence between frequency-domain parameters and time-domain ones is shown using Parseval's theorem. Conclusions are illustrated by numerical examples.

A novel formulation of time-domain antenna parameters and using Parseval's theorem to show the correspondence between mean-value time-domain parameters and mean-value frequency-domain ones are the original contributions of this paper.

Key-Words: method of moments, time-domain, frequency domain, broadband parameters, antennas.

1 Introduction

Launching new entertainment and communication services (digital TV broadcasting, teleconferences, etc.), broadband components of the communication chain have to be carefully designed and selected. In the design and selection process, very important role is played by a proper characterization of electronic devices, including antennas. In this paper, antennas are used as a prototype component we exploit for explaining principles.

All the well-known antenna parameters (directivity pattern, gain, input impedance, etc.) are formulated in the frequency domain [1]. If the communication components are going to be characterized in detail in a wide band of frequencies, respective physical quantities have to be measured or computed on a huge number of harmonics. Such an approach might be laborious and time demanding [2]. Details are given in Section 2 of this paper.

In the last decade, attention is turned to the time-domain approaches to computing and measuring parameters of broadband structures. Exciting a structure a by narrow-enough Gaussian pulse, behavior of the investigated structure can be characterized within a single run of computation or measurement [3], [4]. Due to the conventional understanding of antenna parameters in the frequency domain, results of the time-domain analysis or measurement are usually transformed to the frequency domain using fast Fourier transform, and antenna parameters are then evaluated for each separate harmonics by the usual methods. Such a way, advantages of time-domain analyses or measurements might be significantly depressed [5].

Scanning papers on the time-domain characterization, which were published in the last decade, few relevant contributions were found:

- In [6], time-domain results were used for computing antenna gain, directivity pattern and input impedance directly in the time domain evaluating mean values of

physical quantities and producing mean-value antenna parameters.

- In [7], time-independent parameters of transmitting antennas and receiving ones were formulated computing the autocorrelation of time-dependent quantities; parameters are of the energy-gain nature.
- In [8], a detailed comparison of time-domain directivity patterns and frequency domain ones was given.
- In [9], an analytical formulation of the time-domain reflection coefficient for a conductive half-plane is derived. In [11], an analytical formulation of the time-domain surface impedance for a lossy half-plane is given.

Considering the above-given survey, we can conclude:

- Except of directivity patterns [8], no paper discuses temporal formulation of time-domain parameters. Analytical formulations of the time-domain reflection coefficient [9] and the time-domain surface impedance [11] are valid for half-planes only.
- No paper discuses the exploitation of Parseval's theorem for comparing mean-value antenna parameters in both the domains. Nevertheless, the approach is very similar to the autocorrelation formulation given in [7].

In Section 3, we discuss a possible temporal formulation of antenna parameters. In Section 4, we compare time-domain parameters and frequency-domain ones using Parseval's theorem. Section 5 concludes the paper.

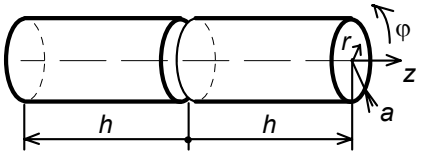

Fig. 1 Symmetrical wire dipole as a canonical testing structure.

For simplicity, we chose a symmetric wire dipole oriented into the *z*-axis of the Cartesian coordinate system as the canonical testing structure (Fig. 1). The antenna is excited by the uniform plane wave (electric field intensity oriented into the *z* direction), which propagates perpendicularly with respect to the antenna axis. The antenna is placed in vacuum.

The antenna is analyzed to obtain current distribution in both the domains. Current distribution is processed to directly obtain antenna parameters in the respective domain.

In numerical simulations, we assume the dipole length $2h$ = 1 m, the antenna radius a = 1 millimeter, perfect conductivity of the antenna wire and free-space surrounding.

2 Frequency Domain

The antenna is numerically analyzed by the standard method of moments [12]: the antenna wire is divided into N_z = 200 one-dimensional segments, currents on segments are approximated by a piecewise-constant function, residual error is minimized applying Dirac pulses as weighting functions. Frequency-domain analysis is performed from 7.5 to 3 000 MHz with frequency step 7.5 MHz. As a result, we obtain column vector of currents on antenna segments for the angular frequency ω of the analysis

$$\mathbf{I}(\omega) = \left[I_1(\omega) \quad I_2(\omega) \quad \dots \quad I_{N_z-1}(\omega) \right]^{\mathrm{T}} , \quad (1)$$

where N_z is the number of the antenna segments and $^{\mathrm{T}}$ denotes the transpose.

From the current distribution, we can evaluate the far-field directivity pattern

$$E_\vartheta(\omega,\vartheta) = \frac{\mu_0 \Delta_z \omega}{2\lambda(\omega)} \frac{j \exp\left[-j k(\omega) r\right]}{k(\omega) r} \sin(\vartheta) \cdot \sum_{n_z=1}^{N_z-1} I_{n_z}(\omega) \exp\left[-j k(\omega) \Delta r_{n_z}\right] , \quad (2)$$

the gain of the dipole in the direction ϑ

$$D(\omega,\vartheta) = 2 \frac{\left|E_\vartheta(\omega,\vartheta)\right|^2}{\sum_{n_\theta=0}^{180} \left|E_\vartheta\left(t,\theta_{n_\theta}\right)\right|^2 \sin\left(\theta_{n_\theta}\right) \Delta\theta} , \quad (3)$$

and the input impedance of the antenna

$$Z(\omega) = U_{feed}(\omega) / I_{feed}(\omega) . \quad (4)$$

All the parameters are related to the canonical antenna on the specific angular frequency ω.

In the relations (2) to (4), ϑ and r are the coordinates in the spherical coordinate system (ϑ is an angle from the antenna axis, r is the distance between the center of the coordinate system and an observation point), ω denotes angular frequency of the analysis, λ is the corresponding wavelength and k denotes the corresponding wavenumber, μ_0 is permeability of

vacuum and j denotes the imaginary unit. Further, Δ_z denotes the length of the antenna discretization segment (all the segments are of the same length), $I_{nz}(\omega)$ is the current on the segment no. n_z, and Δr_{nz} denotes the space shift of the wave radiated by the segment no. n_z and the segment no. n_1. The symbol $\Delta\theta = 1° = (\pi/180)$ rad denotes the angular step in numerical integration in the denominator of (3). Finally, $U_{feed}(\omega)$ and $I_{feed}(\omega)$ are voltage and current on the feeding segment of the dipole on the angular frequency ω.

When computing currents in relations (2) to (4), we divided the antenna wire to $N_z = 19$ segments and we repeated the analysis 400 times (from 7.5 MHz to 3 000 MHz with the frequency step 7.5 MHz). Performing the analysis in MATLAB 6.1 on a regular PC (AMD Athlon XP 2000+, 512 MB RAM, MS Windows 2000), computations consumed (16.69 ± 0.02) seconds of CPU-time.

Substituting computed currents to (2), we can evaluate normalized directivity patterns on specified frequencies (see Fig. 2).

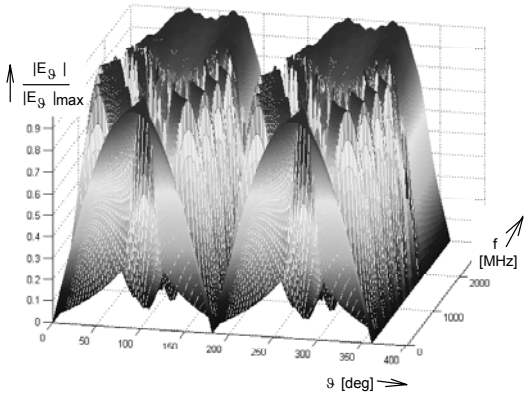

Fig. 2 Normalized directivity patterns of the canonical structure for the whole investigated frequency band.

Substituting computed currents to (3), antenna directivity can be computed for the direction, which is perpendicular to the antenna axis ($\vartheta = 90°$ or $\vartheta = 270°$). The computed directivity is depicted in Fig. 3.

Comparing Fig. 2 and Fig. 3, we can observe an obvious correspondence: the gain reaches maxims on frequencies, on which the main lobe is oriented to perpendicular direction with respect to the antenna axis. If there is null of the pattern in the specified direction, gain is of zero value also.

Substituting computed currents to (3), we can evaluate impedance characteristics of the antenna (see Fig. 4).

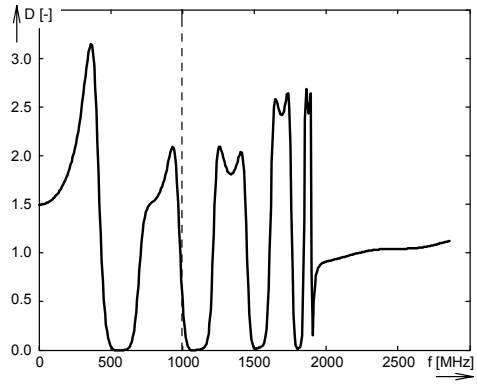

Fig. 3 Directivity of the canonical structure in the direction perpendicular to the antenna axis for the whole investigated frequency band.

Frequency dependencies of directivity patterns, gain and input impedance seem to be realistic by the frequency $f_{crit} = 1\,000$ MHz. On upper frequencies, parameters do not meet the theory.

The problem is caused by the fact that the ratio of antenna segment length to wavelength varies from $1.25 \cdot 10^{-3}$ on the lowest frequency $f_{min} = 7.5$ MHz to $500 \cdot 10^{-3}$ on the highest frequency $f_{max} = 3\,000$ MHz. On the critical frequency $f_{crit} = 1\,000$ MHz, the ratio is $167 \cdot 10^{-4}$. Recommendations given in [12] require the ratio being lower than $100 \cdot 10^{-4}$.

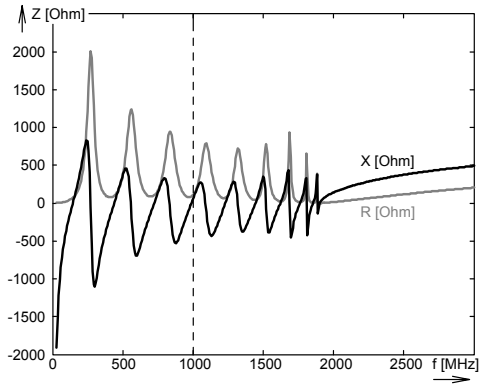

Fig. 4 Input impedance of the canonical structure for the whole investigated frequency band.

In order to overcome this difficulty, adaptive mesh refinement related to the frequency of the analysis has to be implemented. Such a procedure increases CPU-time demands of the computation, of course.

3 Time Domain

The antenna is numerically analyzed by the time-domain integral-equation method [3]. For the analysis, explicit formulation of the method is elected, because:

- Formulation gives more accurate results;
- Discretization step in time has no lower limit, and therefore retarded waves can be computed with an arbitrary accuracy;
- Matrix inverse has not to be computed.

In order to analyze the canonical structure in the identical frequency range with the identical frequency resolution as in frequency domain, the antenna is excited by Gaussian pulse [3]

$$E_{\vartheta}^{I}(\vec{r},t) = E_{\vartheta 0}\,\frac{4}{T\sqrt{\pi}}\exp\left(-\gamma^2\right), \qquad (5)$$

where the coefficient γ is given by [3]

$$\gamma = \frac{4}{cT}\left(ct - ct_0\right), \qquad (6)$$

$E_{\vartheta 0}$ = 120 π V/m is electric field intensity in the origin of the coordinate system, $c = 3 \cdot 10^{-8}$ meters per second is velocity of light. Width of Gaussian pulse has to be set to T = 2 LM in order to excite strong enough harmonics up to 3 GHz (antenna is analyzed in approximately the same frequency range as in the frequency domain). If the antenna wire is divided into N_z = 21 one-dimensional segments (the same discretization as in the frequency domain), the discretization step in time should be chosen as $c\,\Delta t$ = 0.05 LM in order to meet the stability condition. The transients are computed for the time interval T_{tot} = 150 LM, which corresponds to the frequency resolution Δf = 2 MHz (compared to 7.5 MHz in frequency domain).

The abbreviation LM in the above paragraph denotes the light meter [3].

Currents on segments are approximated by a piecewise-constant function, residual error is minimized applying Dirac pulses as weighting functions. As a result, we obtain the column vector of currents on antenna segments for the time instants t of the analysis

$$\mathbf{I}(t) = \left[I_1(t) \quad I_2(t) \quad \ldots \quad I_{N_z-1}(t)\right]^{\mathrm{T}}, \qquad (7)$$

where N_z is the number of the antenna segments and $^{\mathrm{T}}$ denotes the transpose.

From the current distribution, we can evaluate the far-field directivity pattern

$$E_{\vartheta}(t,\vartheta) = \frac{\mu_0\,\Delta_z}{4\pi r}\sin(\vartheta) \qquad (8)$$
$$\sum_{n_z=1}^{N_z-1}\frac{I_{n_z}\left(t+\Delta t-\Delta r_n/c\right) - I_{n_z}\left(t-\Delta t-\Delta r_n/c\right)}{2\Delta t}.$$

Here, the first time derivative of current is approximated by central difference. If the time instant $t \pm \Delta t - \Delta r_n/c$ does not meet the sampling moment, the actual value of current is estimated using linear interpolation between neighboring current samples. The symbol Δt denotes the temporal sampling step, and other symbols were explained before.

On the basis of current distribution (7), gain of the dipole in the direction ϑ can be evaluated according to

$$D(t,\vartheta) = 2\,\frac{\left|E_{\vartheta}(t,\vartheta)\right|^2}{\sum_{n_\theta=0}^{180}\left|E_{\vartheta}\left(t,\theta_{n_\theta}\right)\right|^2\sin\left(\theta_{n_\theta}\right)\Delta\theta}. \qquad (9)$$

Following the approach proposed in Section 2, one might formulate the time-domain input impedance of the antenna as follows:

$$Z(t) = U_{feed}(t)/I_{feed}(t). \qquad (10)$$

In relations (8) to (10), all the temporal parameters are related to the canonical antenna in the specific time instant t.

From the practical point of view, (10) is inapplicable due to the zero samples of current in the feeding gap in the center of the dipole. We therefore convert the feeding voltage $U_{feed}(t)$ and the feeding current $I_{feed}(t)$ into the frequency domain and compute input impedances on respective harmonics (4) in order to determine the frequency range within the time-domain analysis provide accurate results (see Fig. 5).

When computing currents in relations (8) to (10), we divided the antenna wire to N_z = 19 segments and we evaluated 3 150 time samples of current distribution on the antenna (compared to 400 analyses in the frequency domain). Performing the analysis in MATLAB 6.1 on a regular PC (AMD Athlon XP 2000+, 512 MB RAM, MS Windows 2000), computations consumed (19.38 ± 0.02) seconds of CPU time compared to (16.69 ± 0.02) seconds of CPU-time in frequency domain. Hence, demands on computational resources are similar in both the domains.

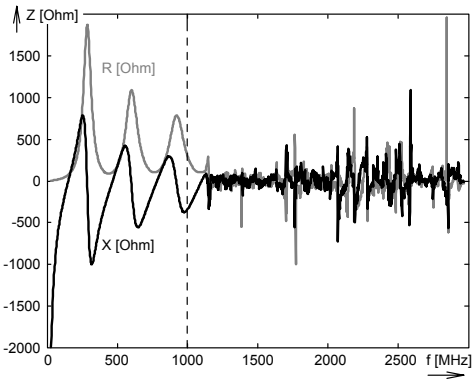

Fig. 5 Input impedance of the canonical structure for the whole investigated time interval when transformed to the frequency domain.

Comparing impedance characteristics based on the frequency domain analysis (Fig. 4) and time-domain analysis (Fig. 5), we can conclude the accuracy of both the approaches is similar.

In Fig. 6, time-domain directivity patterns (relation 8) are depicted for all the iteration steps of the analysis. During the presence of the excitation Gaussian plane wave, the pattern is slightly deformed. Later, maximum of the pattern is oriented to various possible directions except of the antenna axis (see Fig. 2). Since the temporal samples of electric field intensity contain all the excited harmonics, the pattern is corrupted by inaccuracies on higher frequencies.

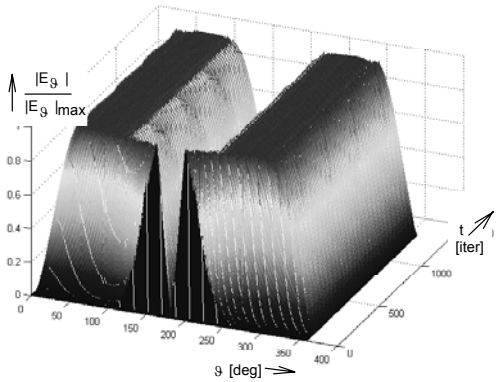

Fig. 6 Normalized directivity patterns of the canonical structure for the whole investigated time interval.

Similar conclusions can be done when computing time course of directivity.

4 Comparisons

Antenna parameters computed in both the domains can be directly compared using Parseval's theorem:

$$\int_{-\infty}^{+\infty} |E_\vartheta(\vartheta,t)|^2 dt = \frac{1}{2\pi} \int_{-\infty}^{+\infty} |E_\vartheta(\vartheta,\omega)|^2 d\omega \ , \quad (11)$$

Integrating electric field intensities from the frequency domain (2) and the time domain (8) over the whole range of analysis, we can obtain mean-value directivity patterns, which have to correspond each other. Observing Fig. 7, differences between mean-value patterns can be detected. Nevertheless, the basic directional behavior of patterns corresponds each other. Detailed explanations of the differences are under intensive investigation at the present.

Similarly, mean-value directivity in both the domains can be defined. For the time domain, we obtain

$$D_{td}(\vartheta) = 2 \frac{\int_{-\infty}^{\infty} |E_{trans}(\vartheta,t)|^2 dt}{\int_0^\pi \int_{-\infty}^{\infty} \left\{ |E_{trans}(\vartheta,t)|^2 \sin\vartheta \right\} dt \, d\vartheta}$$

$$= 1.38 \quad , \quad (12)$$

and for the frequency domain, we get

$$D_{fd}(\vartheta) = 2 \frac{\int_{-\infty}^{\infty} |E_\vartheta(\vartheta,\omega)|^2 d\omega}{\int_0^\pi \int_{-\infty}^{\infty} \left\{ |E_\vartheta(\vartheta,\omega)|^2 \sin\vartheta \right\} d\omega \, d\vartheta}$$

$$= 1.27 \quad , \quad (13)$$

The percentage difference between the results equals to 8.0 %, which can be considered as a satisfactory accuracy.

5 Conclusion

The paper brings the detailed comparisons of time-domain and frequency-domain broadband characterization approaches of communication devices. As a canonical structure exploited to demonstrate the discussed principles, symmetrical wire dipole was used. As the analysis tool, the method of moments in both the domains was applied. Parameters of moment methods were set to provide comparable re-

sults. Both the methods are of similar CPU-time demands.

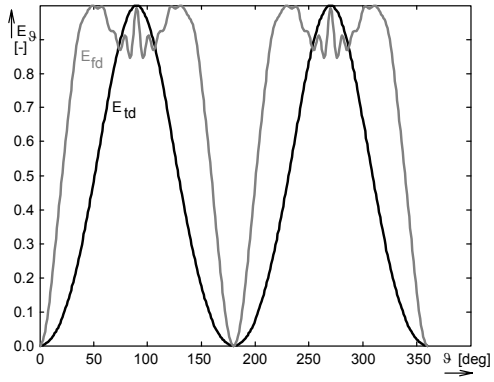

Fig. 7 Comparisons of mean-value directivity of the canonical structure in the direction perpendicular to the antenna axis.

Frequency-domain characterization seems being advantageous thanks to the possible elimination of inaccurate results on higher frequencies. In the time domain, results have to be converted to the frequency domain first, and then, the elimination can be performed.

Analysis results were used to formulate mean-value parameters, and Parseval's theorem was utilized to compare mean-value results in both the domains. Whereas the directivity exhibits a satisfactory correspondence, directivity pattern correspondence shows differences.

Acknowledgements:

Research described in this paper was financially supported by the Grant Agency of the Czech Republic under grants no. 102/04/1079 and 102/03/H086.

Further financial support was obtained from the Czech Ministry of Education under the research programs MSM 262200011 and MSM 262200022.

References:

[1] C. A. Balanis, *Antenna Theory: Analysis and Design*, John Wiley and Sons, 1997

[2] Z. Raida, Z. Škvor, O. Franek, J. Láčík, Z. Lukeš, R. Tkadlec, *Time Domain Modeling of Microwave Structures*. VUTIUM Publishing, 2003 (in Czech)

[3] S. M. Rao, *Time Domain Electromagnetics*, Academic Press, 1999

[4] A. M. Nicolson, C. L. Bennett jr., D. Lamensdorf, L., Susman, Applications of Time-Domain Metrology to the Automation of Broad-Band Microwave Measurements, *IEEE Transactions on Microwave Theory and Techniques*, Vol. 20, No. 1, 1972, p. 3–9.

[5] D. Poljak, C. Y. Tham, *Integral Equation Techniques in Transient Electromagnetics*, WIT Press, 2003.

[6] O. E. Allen, D. A. Hill, A. R. Ondrejka, Time-Domain Antenna Characterizations, *IEEE Transactions on Electromagnetic Compatibility*, Vol. 35, No. 3, 1993, p. 339–346.

[7] A. Shlivinski, E. Heyman, R. Kastner, Antenna Characterization in the Time Domain. *IEEE Transactions on Antennas and Propagation*, Vol. 45, No. 7, 1997, p. 1140–1149.

[8] L. D. DiDomenico, A Comparison of Time Versus Frequency Domain Antenna Patterns. *IEEE Transactions on Antennas and Propagation*, Vol. 50, No. 11, 2002, p. 1560–1566.

[9] E. J. Rothwell, J. Suk, Efficient Computation of the Time Domain TE Plane-Wave Reflection Coefficient. *IEEE Transactions on Antennas and Propagation*, Vol. 51, No. 12, 2003, p. 3283–3285.

[10] G. S. Smith, A Direct Derivation of a Single-Antenna Reciprocity Relation for the Time Domain. *IEEE Transactions on Antennas and Propagation*, Vol. 52, No. 6, 2004, p. 1568–1577.

[11] H. Y. Pao, Z. Zhu, S. L. Dvorak, Exact, Closed-Form Representations for the Time-Domain Surface Impedances of a Homogeneous, Lossy Half-Space. *IEEE Transactions on Antennas and Propagation*, Vol. 52, No. 10, 2004, p. 2659 to 2665.

[12] R. F. Harrington, *Field Computation by Moment Methods*, IEEE Press, 1993.